Novel TM0 Surface Wave Launcher for Integrated Planar Leaky Wave Antennas

Jochen Schäfer, Heiko Gulan, Benjamin Göttel, Thomas Zwick
Institut für Hochfrequenztechnik und Elektronik, IHE
Karlsruher Institut für Technologie, KIT
Karlsruhe, Germany

***Abstract*—In this paper a novel directive TM_0 surface wave launcher for integrated planar leaky wave antennas is presented. As proof of concept the launcher is designed for a frequency modulated continuous wave radar at 120 GHz. Simulations for launcher and antenna are presented, as well as verification measurements of a prototype. Being well matched over the whole WR6 band from 110 GHz to 170 GHz, the designed launcher covers a large bandwidth. The antenna prototype incorporating the new launcher scans over a range of 18° when fed from 110 GHz to 130 GHz.**

I. Introduction

With monolithic microwave integrated circuit (MMIC) technology for the millimeter wave frequency range entering commercialization, very small and cheap radar sensors get possible, like the fully integrated 122 GHz frequency modulated continuous wave radar frontend presented in [1]. Often, not only the distance to a target is of importance, but also the angle of the target towards the radar. Compared to phased arrays or digital beam forming with their increased demand on feed network design and amount of necessary radio frequency (RF) hardware respectively, leaky wave antennas in conjunction with an FMCW radar frontend offer a cheap and efficient way to implement a radar with angle and distance measurement capabilities [2]. Leaky wave antennas radiate in different directions when fed with different frequencies, which is why they are also called frequency scanning antennas. With this characteristic, the antenna performs a scan over the field of view during an FMCW ramp. There are different implementations of leaky wave antennas for different transmission line technologies. In this paper a planar implementation is used, which is inspired by holographic theory [3]. A bound substrate wave in a dielectric slab is used as a reference wave. This wave is excited by a surface wave launcher and in turn excites the hologram, a periodic structure, to radiate a pencil beam to free space. The surface wave launcher is crucial for a good performance, as it is a limiting element for the bandwidth of the antenna. In this paper we evaluate why the TM_0 mode is desirable for an integrated FMCW radar sensor and present a novel TM_0 surface wave launcher enabling the use of the TM_0 mode for this purpose. Simulations and measurements of a prototype (Fig. 1) are presented as proof of concept.

II. System Concept

The antenna is intended for a quasi monostatic FMCW radar at 122 GHz on a layer stack as illustrated in Fig. 3. The main

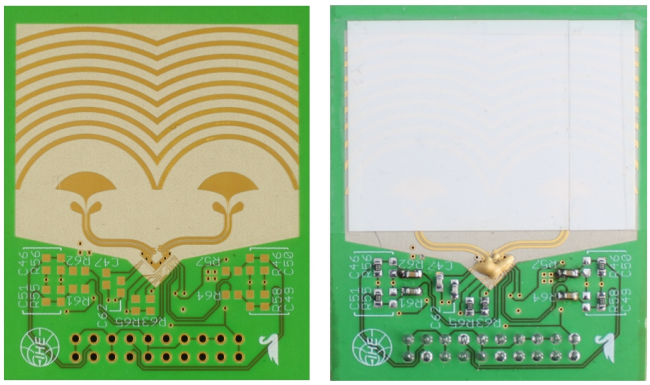

Fig. 1. Two antennas side by side for quasi monostatic FMCW radar. The left picture shows the antenna without the Alumina superstrate, on the right the complete antenna in working condition. The substrate size is 45 mm by 55 mm, the antenna itself is 40 mm by 35 mm large.

RF substrate is a 127 µm thick Rogers 3003 substrate with a permittivity of $\epsilon_r = 3$ and 18 µm copper cladding on both sides. The top copper layer is additionally gold coated for lower loss and corrosion protection. For structural strength and for the baseband electronics, this RF substrate is laminated on a 1 mm thick FR4 substrate with 35 µm copper cladding on both sides. As a superstrate, a 127 µm thick slab of Alumina with a permittivity of $\epsilon_r = 9.9$ is manually attached on top of the upper metal layer after production of the circuit board. Glue is only applied on the outer rim, leaving air between the individual metal traces. The RF components and the antenna are situated on the top layer, whereas power supply and signal conditioning are placed on the bottom side FR4, enabling a high degree of integration and miniaturization, while providing a trade-off between cost and RF attenuation.

Two surface waves are mainly used for leaky wave antennas: The TE_0 and the TM_0 mode. Field patterns are illustrated in Fig. 2. Both modes have no lower cuttoff frequency and are the first modes of their kind that can propagate. Also, both modes can propagate on just a dielectric slab. In this case the TE_0 mode is usually preferred because of the simple excitation by a folded dipole or a Vivaldi antenna [4]. Mode conversion is small and can be neglected. For integrated sensors however, it has the disadvantage that radiation takes place on both sides

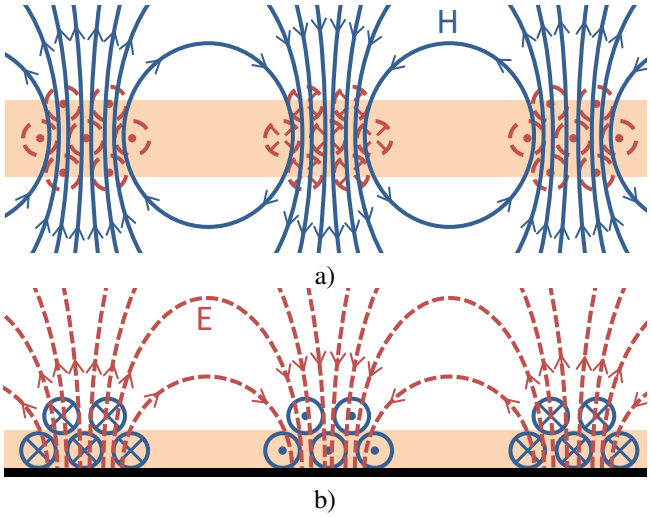

Fig. 2. Illustration of the fields of a TE_0 mode propagating on a dielectric slab (a) and a TM_0 mode propagating on a dielectric slab with backside metallization (b). Both modes propagate to the left.

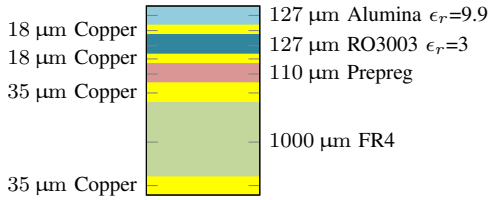

Fig. 3. Layerstack of the target system (not to scale). The superstrate is added manually on top of the top metal after production, leaving air gaps between the stripes.

of the substrate. This means a reflector in a mechanically well controlled distance to the antenna is necessary, which increases manufacturing cost and makes integration more difficult. In contrast to the TE_0 mode, the TM_0 mode can also propagate on a substrate with backside metallization. This allows true single mode propagation and more importantly the metallization then forms an intrinsic shield against the background. This is advantageous because in this configuration the mounting of the antenna does not influence the antenna characteristics and can therefore be neglected during design.

Excitation of TM_0 waves for leaky wave antennas is usually accomplished with a slot antenna in the ground plane, for example a folded dipole slot [5]. This brings two disadvantages: Firstly the shielding towards the backside of the radar is worse, which means the background again influences the antenna behavior. Secondly, the antenna needs to be fed from the backside, so the RF front end needs to sit on the bottom side of the antenna substrate or the RF signal needs to be routed from the top to the bottom layer. This would require vias for RF signals, which would increase manufacturing cost, signal attenuation and design complexity.

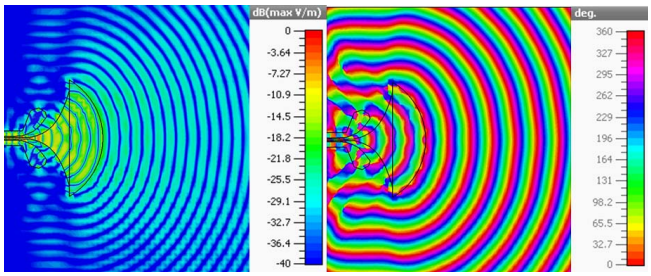

Fig. 4. Simulation results of the proposed feed without a grating at 120 GHz, including the superstrate: On the left the magnitude and on the right the phase of the E-field's z-component.

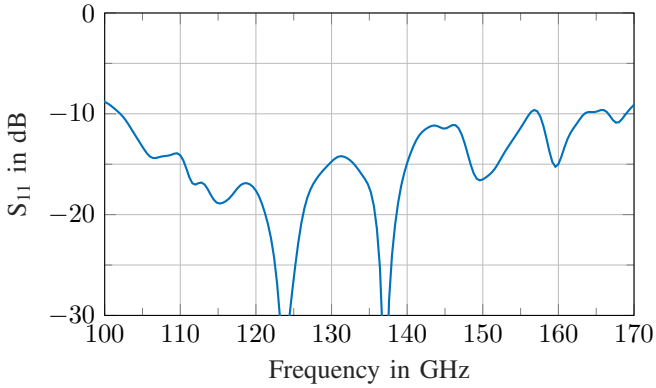

Fig. 5. Simulated reflection coefficient of the feed without a grating.

III. Launcher Design

The new launcher is inspired by the complement of the Vivaldi antenna. Instead of a slot in the ground, the exponential taper is made on the center conductor of a coplanar wave guide with lower ground (CPWG) as can be seen in Fig. 1. The CPWG mode first gradually transforms to a microstrip mode under the tapered center line and then to the desired TM_0 substrate mode. To improve the reflection coefficient and to achieve an undisturbed circular wave front, the aperture of the feed antenna is circular. The z-component of the E-field in Fig. 4 shows a directional radiation of the substrate wave towards the grating and the desired circular phase front. The ground conductors of the CPWG line are gradually retracted from the center conductor for a smooth transition and have round ends to keep spurious radiation low. Due to these measures a high bandwidth can be achieved which can be seen by the reflection coefficient in Fig. 5.

IV. Antenna Grating Design

To validate the suitability of the proposed feed, a grating is necessary to radiate the substrate wave. This grating is designed for the frequency range of 110 GHz to 130 GHz, should radiate to a wide angular range near broadside and should lead to a small beamwidth.
The antenna grating is the radiating element of the leaky wave antenna. Each metal stripe radiates a small amount of the

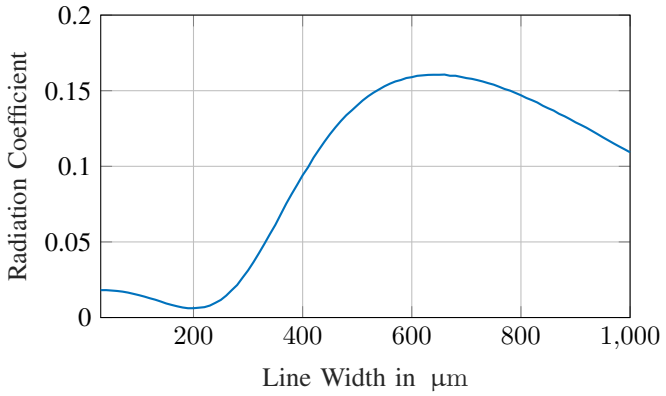

Fig. 6. Radiation coefficient of one metal stripe on Rogers 3003 with backside metallization and a 127 µm thick Alumina superstrate on top of the stripe.

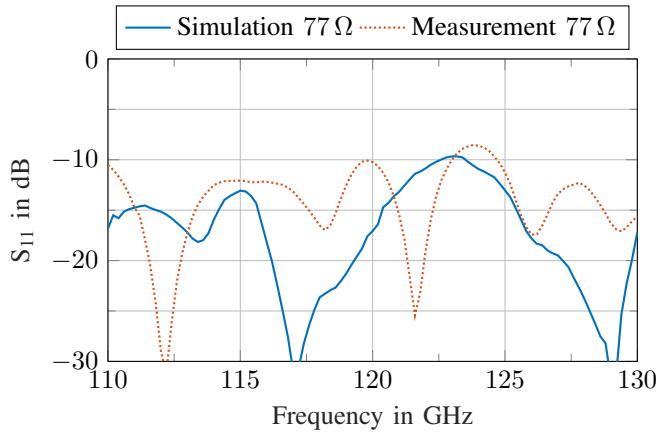

Fig. 7. Simulated and measured reflection coefficient of the antenna prototype as shown in Fig. 1. Both lines are plotted for a reference impedance of 77 Ω.

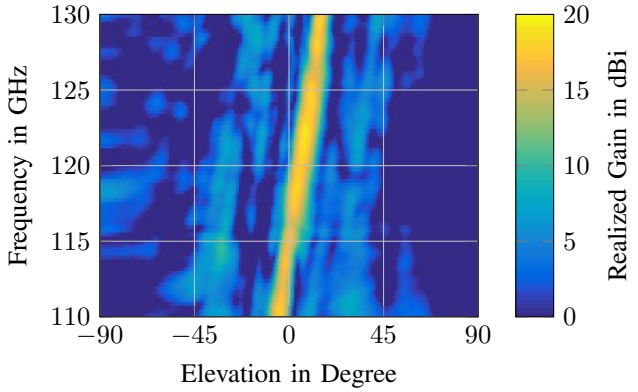

Fig. 8. 2D plot of the simulated antenna pattern. Broadside radiation is at 0°. At smaller angles the main beam tilts towards the surface wave launcher.

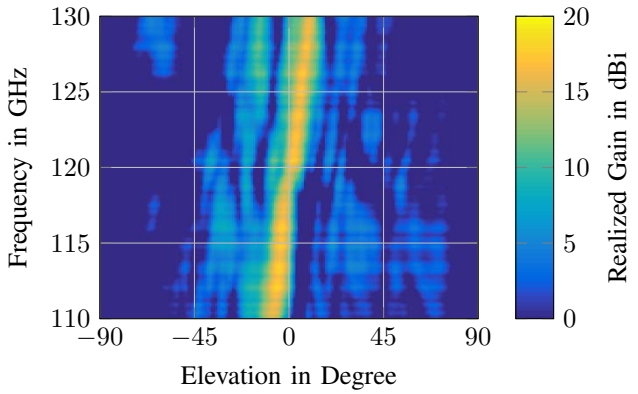

Fig. 9. 2D plot of the measured antenna pattern. Broadside radiation is at 0°. At smaller angles the main beam tilts towards the surface wave launcher.

surface wave. Due to the periodicity of the grating, a specific floquet mode is excited. This mode has a phase velocity higher than the free space phase velocity and therefore radiates. Because the physical periodicity remains constant while the wavelength changes with a frequency change, the radiation direction changes with frequency. Therefore, the periodicity in conjunction with the propagation constant β of the reference wave determines the angle in which the antenna radiates. The angular range that can be scanned with the antenna increases with the permittivity of the substrate material. The use of a high permittivity substrate however, also increases the losses in the RF circuit due to undesired substrate waves. The substrate used for the radar system has a low permittivity of $\epsilon_r = 3$ which results in a small scan range. This is improved by using the high permittivity superstrate over the antenna feed and grating, improving the scan range to 20°. Also, the high permittivity of the superstrate leads to a concentration of the field around the grating, which improves the radiation behavior, because the metal stripes can more effectively short the E-fields. With the superstrate only being over the antenna part of the system, another advantage is the attenuation of spurious substrate waves in the rest of the system because spurious substrate waves are bound to the area with the higher permittivity due to the difference in wave impedance of the modes inside and outside the area of the superstrate.

The width of the stripes is the main parameter for the amount of energy which is radiated by each stripe. The more energy each stripe couples out, the higher the efficiency of the antenna. This is because the surface wave propagates less in the lossy dielectric substrate. A high radiation coefficient also decreases the size of the aperture because all energy of the substrate wave is radiated after less stripes. The downside of this increase in electrical and aperture efficiency is a larger main beam.

Fig. 6 shows the radiation coefficient for different stripe widths of the grating. The coefficients are extracted from simulations of a unit cell with a single grating stripe. Dielectric and metal losses are neglected due to the small size of the simulation cell. Therefore, all losses determined by $L = 1 - |S_{11}|^2 - |S_{21}|^2$ can be attributed to radiation. For the prototype antenna a small beamwidth and a small aperture are requested, so the line width is chosen to be 700 µm. The residual power at the end of the grating should be below

$-10\,\mathrm{dB}$ to avoid a sidelobe caused by the reflection of residual power at the end of the substrate. For a linewidth of $700\,\mu\mathrm{m}$ this is the case for a minimum of 8 stripes. To be on the safe side 9 stripes are used for the antenna, theoretically resulting in $-12.5\,\mathrm{dB}$ residual power. The periodicity of the antenna is chosen to $1900\,\mu\mathrm{m}$ so that the main beam scans close to broadside from $-6°$ to $14°$ when fed from $110\,\mathrm{GHz}$ to $130\,\mathrm{GHz}$. The simulation of the antenna pattern is plotted in Fig. 8 showing the expected scan range of $20°$ and a realized gain of $15\,\mathrm{dBi}$ to $19\,\mathrm{dBi}$. The main lobe $3\,\mathrm{dB}$-beamwidth is $7°$ on average and the sidelobe suppression is better than $-10\,\mathrm{dB}$ above $118\,\mathrm{GHz}$ and better than $-7\,\mathrm{dB}$ in the frequency range below. Sidelobe suppression can be improved by an amplitude distribution realized by using different stripe widths according to the radiation coefficients from Fig. 6. However, at the cost of a wider main beam and a larger aperture.

V. Experimental Setup and Results

Due to the minimum feature size allowed for the manufacturing, the impedance of the pads to contact the antenna cannot be lower than $77\,\Omega$, so the antenna cannot be matched to the $50\,\Omega$ impedance of the measurement system. Therefore, the measurements are renormalized to $77\,\Omega$ in post processing. For the radar system this is not a problem, because the wire bonds used to connect antenna and RF front end can be used to match the connection. The reflection coefficient and antenna pattern are measured on a probe based antenna measurement system [6]. The measured antenna pattern can be seen in Fig. 9. The results are close to the simulated values. The scan range is shifted slightly by $5°$ so the antenna scans from $-9°$ to $9°$. With a small exception at $124\,\mathrm{GHz}$ the antenna is matched better than $-10\,\mathrm{dB}$ as shown in Fig. 7. This could be improved by an amplitude distribution. The reflection at the first stripe is dominant, so with a smaller first stripe reflection would be lower. In Fig. 10 the realized gain of the antenna is shown. The strong ripple on the measurement is attributed to the mismatch between antenna and measurement system. On average the antenna gain is very constant across the bandwidth slightly exceeding the simulated gain at the lower frequencies and slightly falling below near the center frequency. This is probably also due to the general shift between simulation and measurement. Based on simulations the shift is expected to be caused by a small air gap between top metal and superstrate, which slightly changes the propagation velocity. This uncertainty could possibly be avoided by using a superstrate that can be laminated onto the antenna during production, instead of applying the superstrate manually.

VI. Conclusion

The novel Vivaldi type TM_0 surface wave launcher enables the use of integrated leaky wave antennas of the holographic principle for radar applications. The launcher is able to feed the grating over a large bandwidth potentially covering a wide angular range. The measurements of the presented prototype prove the viability of the new feed concept. Improving the resilience to manufacturing tolerances during superstrate application appeared as a topic for further research.

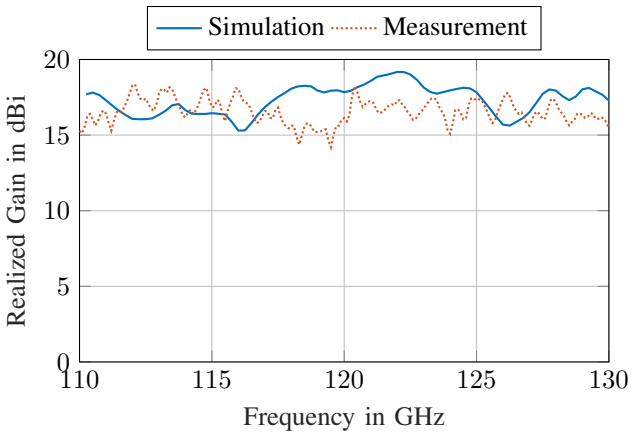

Fig. 10. Realized gain of the antenna across the frequency range

Acknowledgment

The authors would like to thank Robert Bosch GmbH for manufacturing the PCB for the prototype.

References

[1] M. G. Girma, S. Beer, J. Hasch, M. Gonser, W. Debski, W. Winkler, Y. Sun, and T. Zwick, "Miniaturized 122 GHz system-in-package (SiP) short range radar sensor," in *2013 European Radar Conference*, Oct 2013, pp. 49–52.

[2] W. Mayer, M. Wetzel, and W. Menzel, "A novel direct-imaging radar sensor with frequency scanned antenna," in *Microwave Symposium Digest, 2003 IEEE MTT-S International*, vol. 3, June 2003, pp. 1941–1944 vol.3.

[3] C. Rusch, J. Schäfer, H. Gulan, P. Pahl, and T. Zwick, "Holographic mmW-Antennas With TE0 and TM0 Surface Wave Launchers for Frequency-Scanning FMCW-Radars," *IEEE Transactions on Antennas and Propagation*, vol. 63, no. 4, pp. 1603–1613, April 2015.

[4] C. Rusch, S. Beer, H. Gulan, and T. Zwick, "Holographic antenna with antipodal feed for frequency-scanning radar," in *2013 IEEE Antennas and Propagation Society International Symposium (APSURSI)*, July 2013, pp. 234–235.

[5] S. K. Podilchak, A. P. Freundorfer, and Y. M. M. Antar, "Surface-Wave Launchers for Beam Steering and Application to Planar Leaky-Wave Antennas," *IEEE Transactions on Antennas and Propagation*, vol. 57, no. 2, pp. 355–363, Feb 2009.

[6] S. Beer and T. Zwick, "Probe based radiation pattern measurements for highly integrated millimeter-wave antennas," in *Antennas and Propagation (EuCAP), 2010 Proceedings of the Fourth European Conference on*, April 2010, pp. 1–5.